

# Chapter 11

## The HYDRO Software Suite for the Prediction of Solution Properties of Rigid and Flexible Macromolecules and Nanoparticles

José García de la Torre

**Abstract** With basis on the classical concept of bead modeling of polymer hydrodynamics, the HYDRO suite of computer programs allows the calculation of solution properties of macromolecules and nanoparticles of any conformation. Bead or bead/shell models are employed to describe arbitrarily shaped rigid particles, and bead-and-spring models can be used for flexible entities. In addition to general-purpose programs, like HYDRO++, the HYDRO suite contains other programs for calculations starting from specific types of structural information, like atomic or residue coordinates (HYDROPRO, HYDRONMR), or 3D density maps from cryoelectron microscopy (HYDROMIC), or other types constructed by the user (HYDROSUB, HYDROPIX). The programs intended for flexible entities are devised in such a way that they can be applied to a variety of problems, from the simple case of semiflexible wormlike chain to complex structures like those of partially disordered proteins. We provide hints on how the topology and partial flexibility of the structures can be represented by springlike connectors. The HYDRO suite contains also some tools to perform optimization of structural parameters by comparison of calculated and experimental data.

**Keywords** Hydrodynamic properties • Bead modeling • HYDRO programs • Flexible macromolecules • SIMUFLEX

### 11.1 Introduction

#### 11.1.1 A Broad Overview

The purely theoretical work of Albert Einstein made it possible to obtain some information on the geometric size of molecules and colloidal/nanoparticles from

---

J. García de la Torre (✉)

Departament of Physical Chemistry, Regional Campus of Excellence Mare Nostrum, University of Murcia, 30071 Murcia, Spain

e-mail: [jgt@um.es](mailto:jgt@um.es)

properties in dilute solution/suspension, and Jean Perrin added further theory to account for particle shape. Later on, Kirkwood and Zimm, among others, provided insights regarding how to include flexibility in the theories concerning the relationship between structure and dilute solution properties. It was later, in the late 1960s, when Bloomfield et al. (1967) made their seminal contribution to account for the details of biomolecular structure that were emerging by that time, so proposing the so-called bead modeling methods. In a previous chapter in this book, Byron presents a clear overview of the antecedents and present status of this field. In this chapter, I shall concentrate in (i) some essential aspects of bead modeling, (ii) how it has been successfully implemented to describe from very rough to very detailed rigid macromolecular and nanostructures in the prediction of hydrodynamic and other solution properties, (iii) how that treatment can be naturally integrated with conformational statistics in order to describe the effects of flexibility, and (iv) further procedures to attack the “inverse problem,” i.e., how to extract structural information from solution properties.

### ***11.1.2 The Various Kinds of Bead Modeling***

The origins of the bead modeling can be placed in the works of Kirkwood and coworkers about describing either flexible (Kirkwood and Riseman 1948) or rigid polymer chains (Kirkwood and Auer 1951) as a string of beads, i.e., centers of frictional resistance behaving in terms of the Stokes' law for isolated spheres and the Oseen's descriptions of hydrodynamic interaction (HI). The next milestone was set by V. A. Bloomfield et al. (1967), who combined their physical insight with the nascent field of scientific computing. Furthermore, essential theory on hydrodynamic interaction (HI) was developed mainly by Rotne and Prager (1969) and Yamakawa (1970), whose improvements and hinted applicability to rigid particles (Yamakawa and Yamaki 1972; Yamakawa and Tanaka 1972) were the basis for further developments by McCammon and Deutch (1976), Nakajima and Wada (1977), and Bloomfield and García de la Torre (1977a) of advanced bead modeling procedures. In 1981, the last two authors wrote a review of bead modeling describing such further developments in theory and computational procedures (García de la Torre and Bloomfield 1981).

As proposed by Bloomfield et al. in the 1960s, there are two versions of bead modeling. In bead modeling in the strict sense, the purpose is reproducing the size and shape as an array of beads with as few beads as possible. In bead/shell modeling (Bloomfield and Filson 1968), a large number of small beads are used to describe in detail just the surface of the particle, which is where frictional forces really act (Fig. 11.1). Bead and bead/shell models for a variety of macromolecular structures are displayed in Fig. 11.2. For a review and comparison of the modeling strategies, see Carrasco and García de la Torre (1999a). In a recent paper, McCammon and coworkers have presented a detailed appraisal of bead modeling methods (Wang et al. 2013).

**Fig. 11.1** Schemes of (*left*) a bead model in (strict sense) and (*right*) a bead/shell model



In bead modeling in the strict sense, the particle is represented by an array of a moderate number,  $N$ , of frictional elements, such that the size and shape of the array match sufficiently that of the actual particle. On the other hand, bead/shell modeling intends a more detailed representation of the shape, describing its surface – which is where hydrodynamic friction takes place – as a shell of a sufficiently large number,  $N$ , of small frictional elements (“minibeads”).

In bead modeling, the computing time needed for the solution of the hydrodynamic interaction equations is of the order of  $N^3$ , so that the importance of  $N$  in the model is obvious. By the way, the same happens with the number of elements in finite element modeling (Allison 1998, 1999; Aragón 2004). We recommend the use of a range of decreasing minibead sizes and therefore increasing minibead number, from  $N \cong 400$  up to  $N \cong 2000$ . Thus, extrapolation to zero minibead size is made within the computational procedures, therefore obtaining what would correspond to a smooth surface.

The obvious drawback of computation cost has been addressed in the latest versions of the HYDRO suite having recourse to high-performance computing (HPC) techniques. Thus, a shell calculation with  $N \cong 400$ –2000 as it is the case of most of the HYDROxxx programs takes typically less than 10 s in an inexpensive personal computer (the term “HYDROxxx” is used here to represent the suite of HYDRO programs available).

### 11.1.3 Coarse-Grained, Mesoscale, and Multiscale Modeling

Single-valued solution properties, such as hydrodynamic coefficients or the radius of gyration, are obviously related to the low-resolution structure of the solute. Thus, it is certainly justified that the polyhedral head of the T2 virus is represented in Fig. 11.2b by a single bead and its tail a string of beads. As another example, the hydrodynamic properties of an IgG antibody may be influenced by the length of the hinge and the relative size, shape, and disposition of the three subunits but will have little influence of the fine (atomic) details of the protein structure. Thus, a very coarse-grained model bead model (Fig. 11.2c), or a shell model with subunits represented as ellipsoids (Fig. 11.2d), may suffice.

The advent of computational power and availability of high-resolution structures motivated some change of view point in macromolecular dynamics, which evolved to atomic-level descriptions. For some time, single-valued properties characterizing the global dynamics, such as the sedimentation coefficient, were somewhat underestimated, and internal dynamics was approached by atomistic molecular dynamics simulation. Certainly, atomic-resolution structures of globular proteins and nucleic

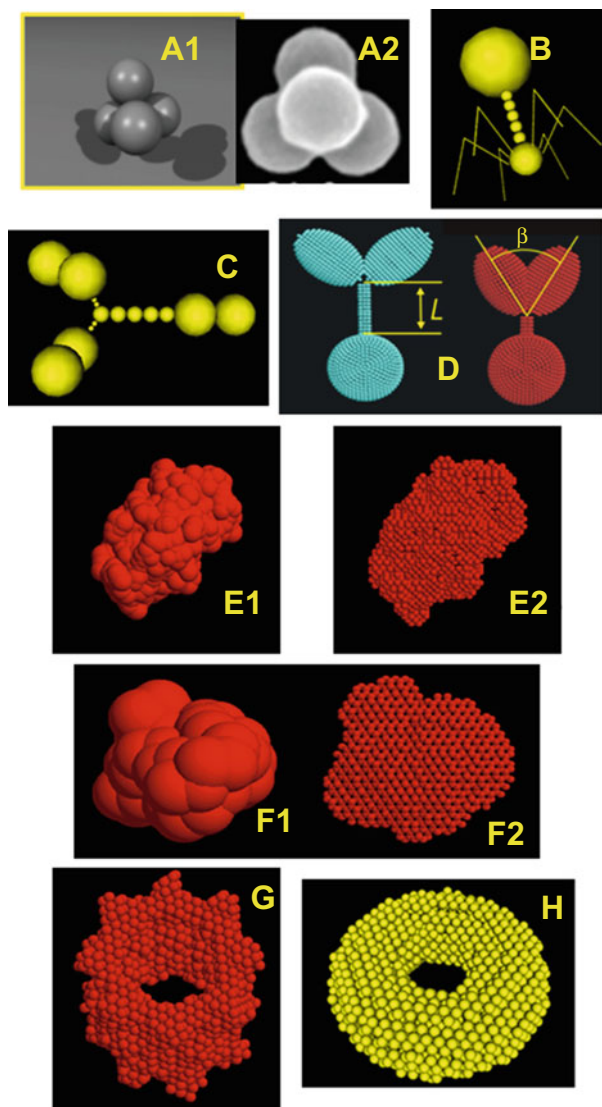


**Fig. 11.2** A gallery of bead and bead/shell models. **(a1)** Simplified bead model for a tetrameric structure, **(a2)** as it is indeed found in oligomeric clusters of nanoparticles. **(b)** Bead model for a bacteriophage virus (García de la Torre and Bloomfield 1977b). **(c)** Simplified bead model for a long-hinged IgG antibody (Gregory et al. 1987). **(d)** Mesoscale shell model for antibodies with varying hinge length and subunit arrangement (Amorós et al. 2010). **(e1)** Primary bead model for lysozyme, with one bead per atom, and **(e2)** its derived shell model (García de la Torre et al. 2000a). **(f1)** Primary bead model for BPTI, with one bead per residue, and **(f2)** its derived shell model (Ortega et al. 2011a). **(g)** Shell model for a large protein, chaperonin (CCT), derived from electron microscopy (García de la Torre et al. 2001). **(h)** Shell model for a geometric object: a doughnut-shaped toroid representing a small cyclodextrin molecule (García de la Torre 2001b; Pavlov et al. 2010)

acids are an attractive starting point for predicting solution properties; this is indeed the aim of our HYDROPRO program (García de la Torre et al. 2000a; see Table I in this reference for a review of previous work). Nowadays, it is widely acceptable that such level of structural detail is not capable to describe relevant dynamic events that take place in a long-time scale (or it is just unnecessary in some instances). The present trend is a return to more coarse-grained models, perhaps not as coarse as in the primitive applications. Thus, model elements may represent not atoms but residues, e.g., amino acid or nucleotide residues, or monomers in polymers. This kind of mesoscale representation, with a medium but still very appreciable resolution, saves much computational effort and is still useful in most instances. The book edited by Voth (2009) provides a number of examples. Still, available procedures for atomistic simulation may be useful for predicting properties of the residues or monomers. Thus, the two approaches are employed in what is presently named multiscale modeling, in which the parameters needed for the elements in the coarse-grained model are determined by highly detailed calculation of the entities composing the whole structure. We have employed this approach in rigid bead modeling (e.g., in HYDROSUB) and in the dynamics simulation of flexible chains, as described later in this chapter.

#### ***11.1.4 The HYDRO Suite***

Following the publication of the first version of the HYDRO program for simple bead models (García de la Torre et al. 1994), a number of other tools, first for rigid particles and then for flexible structures, have been integrated in a suite of computer programs for the prediction of solution properties, including also some tools for the analysis of experimental data (García de la Torre 2014). In this chapter I shall review briefly the set of HYDROxxx programs for rigid particles and then describe the more recently published programs for simulation of flexible structures.

### **11.2 Rigid Particles**

The HYDROxxx programs for the prediction of solution properties of rigid structures are all well documented, with user guides and detailed examples. All of them start from some structural specification and provide as results a number of single-valued solution properties, like diffusion and sedimentation coefficient, the five rotational relaxation times, and the intrinsic viscosity, along with other conformational properties, such as the radius of gyration, the longest distance, and even the particle's covolume, which is needed to evaluate the second virial coefficient (García de la Torre et al. 1999). They also provide the scattering form factor and the distribution of distances, which, accepting the limitations of the

models, may be useful as an estimations for light, low-angle X-ray and neutron scattering.

### 11.2.1 *HYDRO++*

The original HYDRO program (García de la Torre et al. 1994) was updated more recently (García de la Torre et al. 2007) in the HYDRO++ version, including more accurate descriptions of hydrodynamic properties (Carrasco and García de la Torre 1999b) for an improved calculation of rotational coefficients and intrinsic viscosities (which in previous versions were affected by an ad hoc correction). Furthermore, the accuracy of HYDRO++ has been tested against exact fluid dynamics results for arrays of beads and experimental data of recently constructed clusters of spherical nanoparticles (Fig. 11.2a).

### 11.2.2 *HYDROPRO and HYDRONMR*

As mentioned above, HYDROPRO was motivated by the availability of detailed, atomic-level structures of biomacromolecules, coded as PDB files, and followed the aim previously hinted by other authors. The program was conceived to be both accurate and easy to use. Essentially the user has just to supply the PDB file with the atomic coordinates and a few trivial properties of solvent and solute. In the first version of the program (García de la Torre et al. 2000a; García de la Torre 2001a), the programs construct first a primary bead hydrodynamic model (PHM) with one bead per residue (Fig. 11.2e1) with radius  $a$  (the present recommended value is 2.9 Å). Then internally the PHM, a bead model with overlapping beads, is replaced by a shell of up to  $N_{\text{beads}} \cong 2000$  minibeads (Fig. 11.2e2) The computing time (presently a few seconds in personal computers) is determined by this  $N_{\text{beads}}$  regardless of the number  $N_{\text{atoms}}$  of atoms in the model. The same procedure and the  $a$  parameter is valid for small oligonucleotides (Fernandes et al. 2002)

The new version of HYDROPRO (Ortega et al. 2011a) maintains the same simple usage, but includes new internal working modes. A novelty is that – in the spirit of present coarse-graining trends – instead of starting with atomic coordinates, in the new modes it just needs the positions of the amino acid residues; the PHM has one bead per residue (Fig. 11.2f1). An obvious advantage is that the program can be still applicable with a lower-resolution structure. Furthermore, this PHM model can be internally processed in two ways (1) being replaced by a shell (Fig. 11.2f2) of up to  $N_{\text{beads}} \cong 2000$ , as before, and (2) can be used for a bead-model calculation. The latter mode, which deals with a model with important bead overlapping, has been made possible by advances in hydrodynamics of multi-sphere systems (Carrasco and García de la Torre 1999b; Garcia de la Torre et al. 2007, 2010b). In the latter case, the number of elements is  $N_{\text{beads}} = N_{\text{residues}}$ . Recalling that the computing time

is proportional to  $N^3_{\text{beads}}$ , it is evident that it presents a computational advantage over the two other shell-model modes with  $N_{\text{beads}} \cong 2000$  when dealing with cases with less 2000 residues, i.e., smaller than  $\sim 200$  kD, which is the case for most medium-sized globular proteins.

A thorough check of the performance of the three HYDROPRO models has been made by comparing predicted and experimental values with an extremely large set of data. A summary of the outcome is presented in Fig. 11.3. The percent error in the hydrodynamic (Stokesian) radius,  $a_T$ , from diffusion or sedimentation, in the hydrodynamic radius (Einsteinian) from intrinsic viscosity,  $a_I$ , and in the equivalent radius of gyration,  $a_G$ , is indicated for a number of proteins ranging from 56 residues (BPTI) to 10428 (70S ribosome). For the whole set of data, we evaluated the typical percent deviations for each property. As it can be appreciated from the examples in Fig. 11.3, all the procedures give similarly low deviations for the various properties and in the whole range of sizes (for more specific information, see Ortega et al. (2011a)). As a summary, I would enunciate two conclusions: (i) prediction of solution properties can be done with coarse-grained residue-level structures with the same quality as those from atomic-level structure, and (ii) for large protein and macromolecular complexes, the shell-model modes of HYDROPRO provide

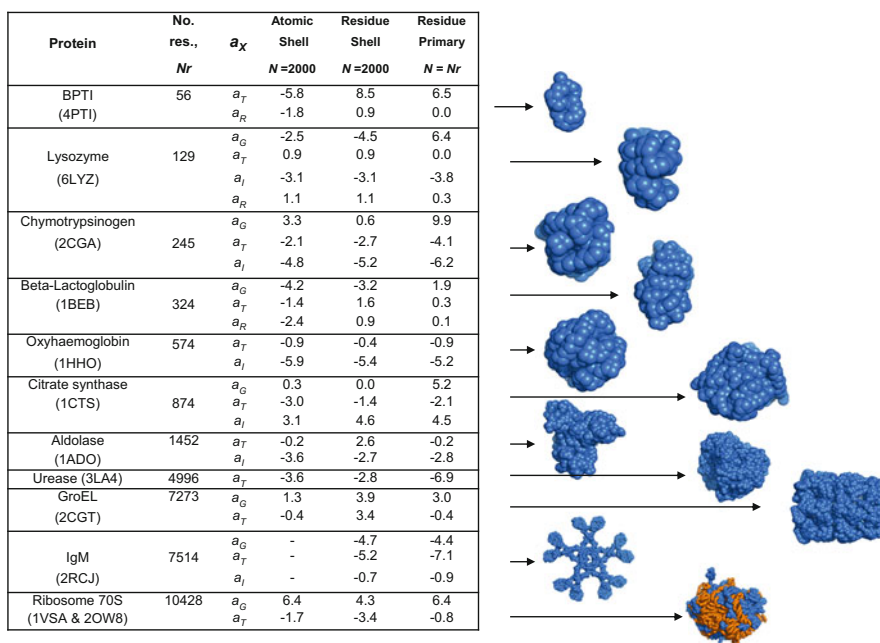


**Fig. 11.3** Percent difference between experimental and calculated Stokesian ( $a_T$ ) and Einsteinian hydrodynamic radii ( $a_I$ ), and radii of gyration ( $a_G$ ), for a selection of proteins of widely different sizes. Calculation modes are (a) atomic PHM,  $a=2.9$  Å, with shell-model calculation; (b) residues PHM,  $a=5.0$  Å, with shell-model calculation; and (c) residues PHM,  $a=6.1$  Å, with bead-model calculation

predictions with similar accuracy and computational requirements as in the case of small proteins, in contrast with other approaches, like that of Rocco and coworkers (Rai et al. 2005; Brookes et al. 2010), for which computing time grows as the third power of the number of atoms or residues and do not seem feasible for proteins larger than a few hundred kD.

As other HYDROxxx programs, HYDROPRO has been benefited by optimization of the computer code and use of high-performance computing techniques that have dramatically reduced CPU time for any structure, regardless of molecular size, to a few seconds in the simplest personal computer. Furthermore, a user-friendly graphical user interface is available, allowing real-time exploration of changes in structures, parameters, etc., with graphical visualization of bead models and numerical results. Although other approaches, with the same aim as HYDROPRO, are available in the literature and, as HYDROPRO, are of public domain, it can be affirmed that our program is the one most widely used. Since the publication of the year 2000 version, it has received over 600 citations, and the 2011 version, 3 years after its publication, is cited in over 80 references. Recently, some authors are devising quite general tools for structural search by means of ambitious global analysis of NMR, SAXS/SANS, and solution hydrodynamics; HYDROPRO has been the choice for the latter purpose in two significant achievements (Bernadó and Blackledge 2009; Krzeminski et al. 2013).

A few words to mention that a sequel of HYDROPRO is the HYDRONMR program (García de la Torre et al. 2000b), specifically intended for predicting residue-specific NMR T1 and T2 relaxation times. These quantities depend not only (as is the case of the five rotational relaxation times) on the size and shape of the rigid particle, but they are also determined on the location and orientation of the amino acid residue within the protein. Thus, the series of T1/T2 ratios along the sequence of the protein contains a large amount of information. As NMR spectroscopy is somehow far from the reach of this book, the reader is referred to the original publication and to the available computer program from more information.

### 11.2.3 *HYDROMIC*

With a purpose similar to HYDROPRO, HYDROMIC (García de la Torre et al. 2001) was conceived to make predictions of solution properties from structures of the (usually large) proteins and macromolecular complexes derived from electron microscopy. Electron-density 3D maps, with a cutoff density, define a 3D shape of the particle. Instead of the PDB atomic coordinates in HYDROPRO, HYDROMIC uses such density map as the primary structural information and, as the first version of HYDROPRO, constructs hydrodynamic bead/shell models for which properties are evaluated (Fig. 11.2g). The use of this tool is not as extended as that of HYDROPRO. Apart from the more limited amount of structural information of this kind, the variety of different formats for the density maps has been a further impediment. HYDROMIC was initially programmed as to work with the “spider”



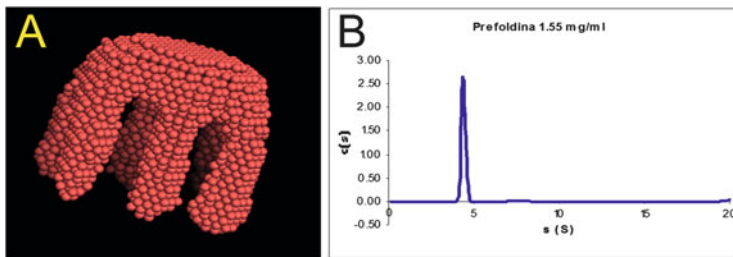


**Fig. 11.4** (a) Shell model constructed by HYDROMIC when processing the 3D EM map of prefoldin. (b) SEDFIT (Schuck 2000) analysis of a sedimentation velocity experiment

format, which was by no means the only one. The latest version included further the common “MRC” format. A public domain tool “em2em” (ImageScience 2014) is available for conversion of other formats.

As a sample of recent application, we advance here results (Ortega et al., to be published) on the experimental and computational characterization of prefoldin, a chaperon protein with a peculiar six-digit hand shape that likely works as an efficient clamp to carry its cargo. With a protein sample and the MRC electron density map, kindly supplied by Prof. J. M. Valpuesta (CSIC, Madrid), we first carried out sedimentation velocity experiments at three concentrations, from 1.55 to 0.19 mg/ml, with both absorbance and interference detection, observing always a sharp peak at  $s_{20,w} = 4.5 \pm 0.1$  S, independent of concentration. The HYDROMIC prediction was  $s_{20,w} = 4.6$  S (Fig. 11.4).

#### 11.2.4 HYDROSUB

The rationale underlying the HYDROSUB (Garcia de la Torre and Carrasco 2002) method belongs to the concept that has been mentioned above as multiscale coarse-graining modeling (we have also sometimes used the term “crystallohydrodynamics”; Carrasco et al. 2001; Lu et al. 2007). The hydrodynamic model is composed by ellipsoids of revolution or cylindrical subunits, which are internally represented by shell models. It presents the obvious advantage of constructing models with nonspherical elements. In applications, it is particularly suited for large multisubunit complexes whose whole structures are not amenable to direct determination (or is just better handled with a coarse-grained representation), while sufficient information is available separately for the subunits. The size and shape of the ellipsoids or cylinders can be fitted from experimental data (Harding et al. 1997; García de la Torre and Harding 2013). Alternatively, if high-resolution diffraction or NMR information is available for the structure of a subunit, a best-fitting ellipsoid can be found from such structure using either COVOL (Harding et al. 1999) or

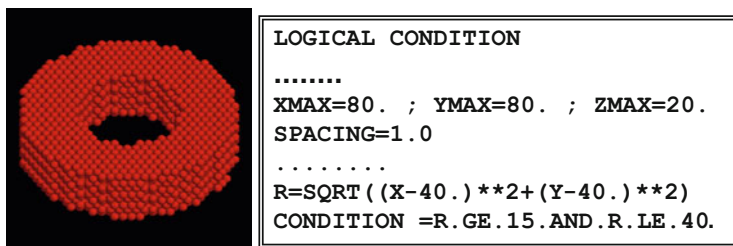


**Fig. 11.5** Lines of Fortran code to be inserted in HYDROPIX for specifying a disk with a hole with inner and outer radii 15 and 40, respectively, and thickness 20. Enclosing boxes have opposite corners at (0,0,0) and (80,80,20). The particle's center is at (40,40,10)

ORIEL (Fernandes et al. 2001). One could even “generate” solution properties using HYDROPRO that would be then retrofitted to get subunit dimensions.

Once the size and shape of the subunits are fixed, the structure of the multisubunit complex is defined by a minimum set of a few geometric parameters that determines their arrangements (Fig. 11.2d). This way makes it possible to carry out predictions of solution properties for this kind of structures in terms of such few geometric parameters or deduce them from the properties using tools that we have also devised (*vide infra*).

### 11.2.5 HYDROPIX

Last but not least, HYDROPIX (García de la Torre 2001b) is a software program that permits the calculation of solution properties for any arbitrarily shaped particle. Instead of being specified by a model of spheres or ellipsoids, the particle is “programmed.” A Fortran source code is provided, within which the user has to insert two pieces of code that (1) gives the coordinates of a box that encloses the particle, the program which fills the box with a cubic lattice, and (2) determines whether or not a point within the box (node in the lattice) belongs to the particle (Fig. 11.5).

## 11.3 Flexible Particles

### 11.3.1 Introduction

As indicated above, bead models were introduced for the characterization of flexible macromolecules. Beads, joined by suitable (either rigid or partially flexible) connectors, were proposed as models for chain macromolecules. In order to develop theo-

ries that would supply analytical expressions for the solution properties, such very coarse-grained models were treated with approximate description of conformational statistics and hydrodynamic interaction. Present textbooks provide pedagogical descriptions of those classical treatments (Rubinstein and Colby 2003; Serdyuk et al. 2007; Hiemenz and Lodge 2007). When computers become accessible, abstract, theoretical work was replaced by computer simulation. A landmark is the proposal by Zimm (1980) of coupling Monte Carlo (MC) simulation with the more rigorous hydrodynamics used for rigid bead models by García de la Torre and Bloomfield (1977a, b). However, by the same time, the availability of computing power was increasing spectacularly, and it was possible to have recourse to computer simulation to solve the problems not accessible to pure theory. A great deal of knowledge on macromolecular dynamics has been achieved by MC methods (Binder 1995). Particularly, the rigid-body Monte Carlo (RBMC) procedure described below has been widely employed to obtain hydrodynamic coefficients and conformational properties of flexible structures ranging from random coils (García de la Torre et al. 1982) to hinged, semiflexible particles (Iniesta et al. 1988) and semiflexible wormlike chains (Amorós et al. 2011).

An alternative for studying, in a rigorous way, every detail of macromolecular hydrodynamics (beyond the limitations of RBMC, *vide infra*) is Brownian dynamics (BD) simulation. In a pioneering paper, Ermak and McCammon (1978) proposed a practical simulation procedure that embodies first principles of Brownian motion with the fluid dynamics concept of hydrodynamic interaction (HI), of which the first applications to macromolecular hydrodynamics appeared in the 1980s (e.g., Allison and McCammon 1984; Diaz et al. 1987). Over the years, improvements of this algorithm and other procedures for DB simulation have been developed; for a recent overview, see Rodríguez Schmidt et al. (2011).

### 11.3.2 A General Bead-and-Spring Model

Like in the bead models for rigid particles, models for flexible entities are composed by beads, which are the elements at which the frictional forces act. We stress here the relevance of using bead models for rigid particles, rather than other descriptions (e.g., Aragón 2004); a large body of knowledge and developments, from concepts to computer codes, for rigid bead models can be used for flexible ones.

The additional ingredients are those intended for representing the intramolecular interactions and the internal degrees of freedom. These will be expressed in terms of interbead potentials in RBMC or forces in BD. The most basic ones are connectors joining neighbor beads that must remain somehow bonded. Rigid, fixed bond-length constraints present some implementation difficulty, and it is generally preferable to

employ “springs,” i.e., bonds of variable stiffness, with the simplest case being the Hookean spring potential:

$$V_{ij}^{(\text{conn})}(l_{ij}; H_{ij}, l_{ij,\text{eq}}) = \frac{1}{2} H_{ij} (l_{ij} - l_{ij,\text{eq}})^2$$

where  $l_{ij}$  is the instantaneous bond length and  $l_{ij,\text{eq}}$  is its equilibrium value. A value of  $H_{ij}$  much greater than  $k_B T / l_{ij,\text{eq}}^2$  ensures that the bond is very stiff; the r.m.s. fluctuation of  $l_{ij}$  is  $(k_B T / H_{ij})^{1/2}$ ; for instance, it is only 10 % if  $H_{ij} = 100 k_B T / l_{ij,\text{eq}}^2$ . A more sophisticated – and more widely applicable potential – is the one accounting for arbitrary spring stiffness and finite extensibility,  $l_{ij,\text{max}}$ , with a potential with three parameters  $V_{ij}^{(\text{conn})}(l_{ij}; H_{ij}, l_{ij,\text{eq}}, l_{ij,\text{max}})$  (del Río Echenique et al. 2009; García de la Torre et al. 2010a).

Angles between two neighbor bonds may be constrained by a bending potential, involving the position of three beads:

$$V_{ijk}^{(\text{ang})}(\alpha_{ijk}; H_{ijk}, \alpha_{ijk,\text{eq}}) = \frac{1}{2} Q_{ijk} (\alpha_{ijk} - \alpha_{ijk,\text{eq}})^2$$

where  $\alpha_{ijk}$  is the angle subtended by the bond vectors  $i \rightarrow j$  and  $j \rightarrow k$  ( $\alpha_{ijk} = 0$  if the vectors are aligned), and  $\alpha_{ijk,\text{eq}}$  is the equilibrium value of this angle. Quasi-rigid bond angles may be determined by a fixed  $\alpha_{ijk,\text{eq}}$  and a sufficiently high value of  $Q_{ijk} / k_B T$ . Another case is the bead-and-connector representation of bending flexibility of wormlike chains; then the equilibrium configuration is straight, and bond lengths have all the same  $l_{\text{eq}}$ , and the force constant is related to the persistence length (Hagerman and Zimm 1981; Allison 1986; Garcia de la Torre 2007), by

$$P = Q l_{\text{eq}} / k_B T$$

while the contour length,  $L$ , is related to the number of quasi-rigid bonds in the discrete bead-and-connector representation as  $L \cong N l_{\text{eq}}$ .

Another essential interaction refers to interaction between nonbonded pairs of beads, which reflect long-range intramolecular interactions. An essential contribution is that from attractive/repulsive van der Waals interactions, usually referred to as excluded volume (EV) effects. The most easy way to account them for is the hard-sphere potential,  $V^{(\text{nonbond})}(r) = 0$  if  $r > r_{\text{cutoff}}$  and  $V^{(\text{nonbond})}(r) = \infty$  if  $r < r_{\text{cutoff}}$ , where  $r_{\text{cutoff}}$  is a distance that can be taken as the sum of some effective radii of the elements. In the case of BD, where the intervention of forces rather than potentials is required, continuous and differentiable potentials are needed. One obvious candidate is the Lennard-Jones potential:

$$V_{ij}^{(\text{nonbond})}(r_{ij}; \epsilon_{ij}, \sigma_{ij}) = 4\epsilon_{ij} \left[ (r_{ij}/\sigma_{ij})^{12} - (r_{ij}/\sigma_{ij})^6 \right]$$

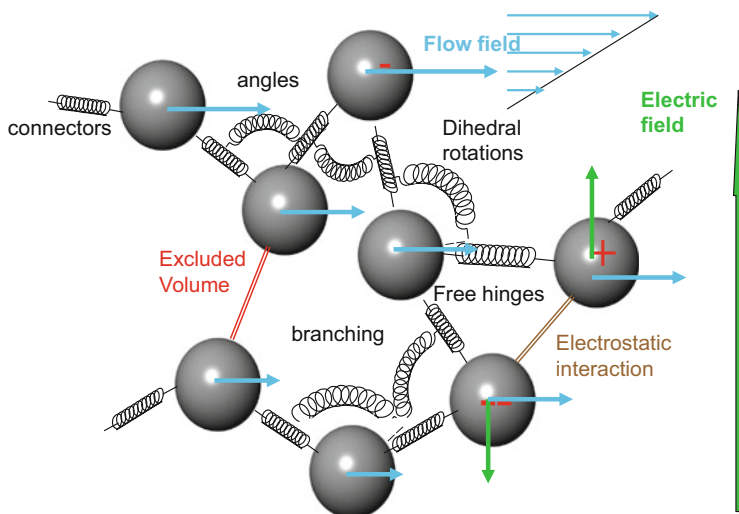


**Fig. 11.6** Schematic representation of a bead-and-connector model for flexible particles with arbitrary topology and diverse intra- and extra-molecular interactions

where  $\varepsilon_{ij}$  and  $\sigma_{ij}$  are the classical Lennard-Jones energetic and geometric parameters, respectively. Many other forms of continuous, differentiable potentials have been proposed in the MC and molecular or Brownian dynamics literature.

Of course, many other intramolecular interactions may be relevant. Such as in the case of electrostatic interactions, usually mediated by the ionic strength of the solvent; a  $V^{\text{(electDH)}}(r)$  can be included by a Debye-Hückel potential between charged beads. The interaction between the molecule in a flow field or its charged elements and dipolar bonds in an electric field may also be included in the model and simulation procedures. Last but not the least, the method is not restricted to the simplest, linear topology; instead, any other (say circular, branched, etc.) can be considered. A general overview of such a general bead-and-connector model is depicted in Fig. 11.6

### 11.3.3 MONTEHYDRO and SIMUFLEX

This general mechanic model is implemented in our programs MONTEHYDRO and SIMUFLEX for flexible particles. The user can choose from a menu including a variety of intramolecular interactions and external agents. MONTEHYDRO (García de la Torre et al. 2005) carries out Monte Carlo simulations and computes overall properties in the MCRB scheme, i.e., as averages over conformations considered as instantaneously rigid. This scheme is somehow approximate (Fixman 1986; Rodríguez Schmidt et al. 2012), but the bias that it may introduce seems appreciable

only for very long and very flexible chains, and in practical instances it is assumed to be of the same order as the uncertainty of experimental data.

However, the neglect of internal dynamics makes MCRB inadequate for the prediction of more detailed, local-scale aspects of macromolecular dynamics. Brownian dynamics (BD) simulation is the most general and rigorous approach (although more complex to carry out and more computationally intensive). Based on the same mechanical model – now in terms of forces, not potentials – BD has been implemented in our package SIMUFLEX (García de la Torre et al. 2009). It actually consists of BROWFLEX, basically a BD simulation engine, and ANAFLEX, which carries out a variety of analysis of the BD trajectories generated by BROWFLEX, from the simple statistics for the mean square displacement of the center or mass, which provides a rigorous evaluation of the diffusion coefficient, to the reorientational correlation times required for NMR relaxation. The overall properties alternatively evaluated by MONTEHYDRO and SIMUFLEX are in good agreement, but SIMUFLEX allows for a direct simulation of the internal dynamics. A nice application of this possibility is the simulation of single-molecule events, such as the different ways on unfolding of a DNA molecule in an elongational flow (Perkins et al. 1997; del Río et al. 2009), or the effect of strong centrifugal forces in an extremely long-chain molecule (like those very long viral DNAs) which produce the so-called anomalous sedimentation consisting of an unexpected effect of rotor speed on the observed sedimentation coefficient (Zimm 1974; Zimm et al. 1976; Schlagberger and Netz 2008).

### 11.3.4 *Examples: Dendrimers and Intrinsically Disordered Proteins*

It seems worth to mention very briefly two recent applications of MONTEHYDRO and SIMUFLEX in two fields of current, intense activity: dendrimers (del Río et al. 2009), as synthetic, polymeric nanomaterials, and intrinsically disordered proteins, a major challenge of present protein biophysics. In both cases, a multiscale approach was followed, avoiding to fit parameters against experimental data; instead, the parameters of the coarse-grained models are extracted from existing structural information or gathered from atomistic simulations, not of the whole molecule but of its constituent entities.

Dendrimers are regularly branched polymers with an absolutely defined topology and molecular size. Branches are small flexible molecular entities having a few chained atoms. One bead and one spring represented each branch. Their effective hydrodynamic radius was evaluated by the RB treatment using molecular dynamics, MD (rather than MC) simulation of a single branch, which was employed also to determine the distribution of end-to-end distance, according to which parameters  $H_{ij}$ ,  $l_{ij,eq}$ , and  $l_{ij,max}$  for  $V_{ij}^{(conn)}$  were fixed. Similarly, MD simulations of a branched trimer were employed to obtain statistic needed to fix the angular parameters

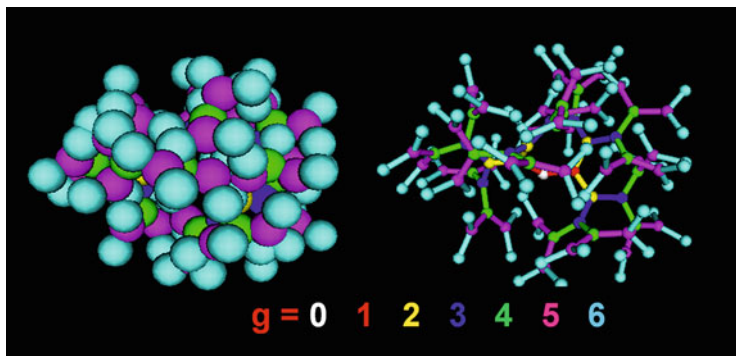


**Fig. 11.7** Snapshot of a sixth-generation dendrimer of mono-polybenzylether with 127 branches (*left* is actual model; at *right*, bead sizes reduced to show the connectors)

$H_{ijk}$ ,  $\alpha_{ijk,eq}$ . In this way, the general mechanic model (Fig. 11.6) for dendrimers is parameterized in an ab initio manner. A snapshot of an instantaneous conformation of a sixth-generation dendrimer is displayed on Fig. 11.7. For four different kinds and various generation numbers, the hydrodynamic radii and radius of gyration were predicted with accuracy of 3–5 %. Furthermore, the BD simulation allows for the simulation of internal dynamics, with greater mobility on going from the inner to the outer branches, which is reflected in NMR relaxation times, and is related to the application of dendrimers in drug encapsulation (García de la Torre, to be published).

We have used the methodology to predict overall properties and internal dynamics of a subclass of intrinsically disordered proteins, in which one can differentiate quasi-rigid domains and flexible linkers or tails. In the coarse-grained model, with one bead per amino acid residues, the linkers and tails are modeled as flexible chains with virtual  $C^\alpha-C^\alpha$  bonds with  $l_{eq} = 3.8 \text{ \AA}$  and  $H$  sufficiently high so that the virtual bond is quasi-rigid. For coherence with the hydrodynamic representation of amino acid residues in HYDROPRO, the hydrodynamic radius of the residue was as there  $6.0 \text{ \AA}$ . Parameters for the angular potential were taken from a statistics of angles between consecutive  $C^\alpha-C^\alpha-C^\alpha$  virtual bonds in the coil regions of proteins (Kleywegt 1997). The excluded volume parameters were taken so that calculations of solution properties of fully disordered (chemically denaturated) proteins were accurately described (García de la Torre, to be published). For the globular, quasi-rigid domains, a special intramolecular potential (the so-called Gō model, Clementi et al. 2000) is employed for the so-called essential pairs (Sobolev et al. 1999).

Several proteins, displayed in Fig. 11.8, were considered in this study. Excellent agreement with experimental SAXS/SANS results was always found for the radius of gyration, and in spite of the coarse-grained modeling, even the scattering intensities and distribution of distances were quite accurately reproduced. For ZipA, the experimental and calculated sedimentation coefficients were 2.2 and 2.1 S, respectively. For BTK, these values were 3.9 and 3.3, with a more deficient

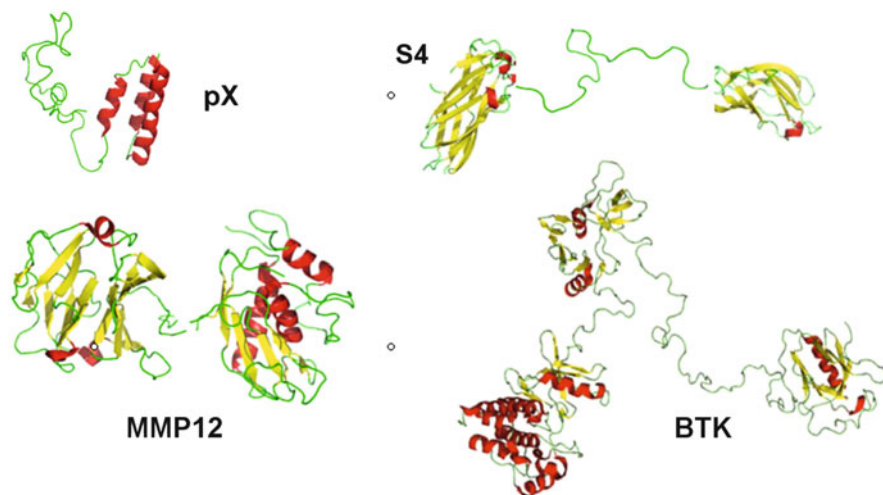


**Fig. 11.8** Snapshots of conformation of some intrinsically disordered proteins

agreement that can be understood considering not only the amount and complexity of the modeling and computational methodology but also the complex structure of the protein itself, with 659 residues structured in four globules connected by four linkers.

### 11.3.5 Wormlike Chains

The Kratky-Porod wormlike chain (WC) is the essential model for many polymers having a continuous stiffness, and its utility encompasses, in addition to the paradigmatic case of double-stranded DNA, most polysaccharides and a number of synthetic polymers. The classical work by Yamakawa and Fuji (1973, 1974) has been for many years the basis for the determination from solution properties of the three essential parameters: the persistence length,  $P$ ; mass per unit length,  $M_L = M/L$ ; and hydrodynamic diameter,  $d$ . However, it is well known that their equations do not cover the whole range of conformations, gauged by the ratios  $L/d$  and  $L/P$ . Thus, it fails for short, thick rods and for long flexible chain is affected by the well-known preaveraging approximation.

Pursuing the description of conformation and dynamics of semiflexible chains and DNA in particular has been an essential purpose of this author for many years (García de la Torre et al. 1975; García de la Torre and Horta 1976). In an attempt to provide a computational framework that would be able to predict solution properties of WCs for the whole range of the parameters, we recently undertook a computer simulation (Amorós et al. 2011), yielding numerical results and a computer program



which have been tested very satisfactorily with experimental data of sedimentation and diffusion coefficients, intrinsic viscosity, and radius of gyration of DNA from 8 to 200,000 base pairs. As we describe later on, this program is the basis for a tool intended for the inverse problem of determining the WC parameters from experimental data.

## 11.4 Global Fitting for Structural Determination: HYDROFIT

An obvious aim of measuring and calculating solution properties of macromolecules and nanoparticles is to obtain information about its structure in solution. Unfortunately, single-valued properties do not convey sufficient information content as to provide detailed structural information. Still, in some cases, the structural search is reduced to the determination of a set of parameters characterizing an assumed kind of structure. The computer programs for calculation of properties could be used in a trial-and-error manner in the search for such parameters. We have developed tools to make the search easy and systematic. A brief summary is presented here; for details, see Ortega et al. (2011b).

### 11.4.1 HYDFIT

The HYDROxxx programs admit the calculation, in a single run, for multiple structures. Users can code ancillary programs for producing the data files, but we have also developed tools like MULTIHYDRO or MULTISUB that facilitate that task. Among the output from the HYDROxxx programs is a file intended to be read by the HYDFIT program, which is in charge of finding the best-fitting structure by comparison with a set of experimental properties. The program works optimally with a varied set of properties, including, say, sedimentation or diffusion coefficients, intrinsic viscosity, radius of gyration, longest distance, etc. Internally HYDFIT seeks to minimize a target function  $\Delta^2$  that measures the square deviations between calculated and experimental results. In order to treat simultaneously different properties in an equilibrated manner, the analysis is made in terms of equivalent radii (Ortega and García de la Torre 2007).

The value  $100\Delta$  is representative as the typical percent error for the whole set of properties.

As a pedagogical example, the HYDFIT user manual describes a hypothetical case in which a double-stranded short DNA oligonucleotide is bent, at a point and with some angle to be determined. The short DNA is modeled as a rigid, bent array of beads. MULTIHYDRO helps in the construction of a series of models in which the position and bent angle are varied. HYDRO++ computes the properties for all

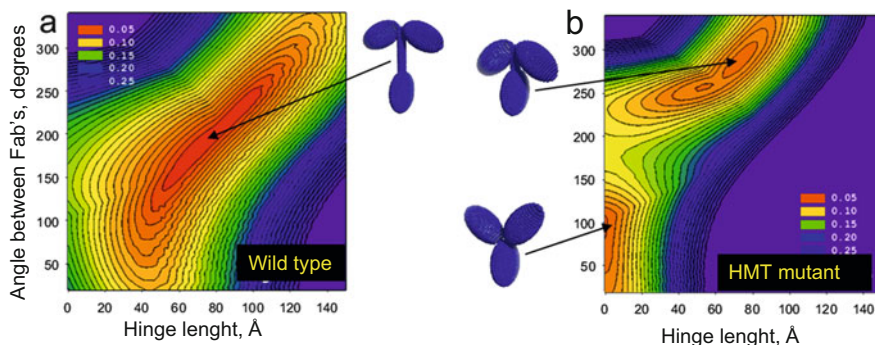


**Fig. 11.9** Contour plots of the target function  $\Delta$  in the HYDROSUB/HYDFIT analysis of two species of antibody IgG3 (*left* wild type, *right* mutant HMT)

the structures in a single run and produces the summary file, which is processed by HYDFIT. The bent position and angle can be unambiguously determined from solution properties.

Another real application has been the determination of the differences between the wild type (WT) of antibody IgG3 and one of its mutants (M15). Coarse-grained, reduced models, in which the essential parameters were the length of the hinge,  $L_h$ , and the angle,  $\beta$ , between the Fab subunits (Fig. 11.2d) were submitted to HYDROSUB calculation. This was done for multiple conformations, with varying  $L_h$  and  $\beta$ , generated by MULTISUB. Then, HYDFIT processed the data searching for minima of  $\Delta$  (Fig. 11.9). The analysis reveals a well-defined conformation for the WT, characterized by a remarkably long hinge. For M15 there are some structures that fit the data with nearly the same deviation (note that the detection of these possible ambiguities is another merit of the HYDROFIT approach), but all are characterized by a much shorter hinge.

### 11.4.2 Multi-HYDFIT

While HYDROFIT is intended for the determination of the structure of a single molecule or sample, Multi-HYDFIT attempts the fit of various properties for a series of samples having in common the same model parameters. Such is the case for a series of samples of a wormlike macromolecule with varying molecular weight, for which various properties may be available. With the same rationale as in HYDROFIT, here again the target function is minimized for the whole series of samples and all the properties in a truly global fit of the WC parameters. A number of examples of using Multi-HYDFIT are provided in the original reference (Amorós et al. 2011; see also the supporting information of this paper). Just to present here

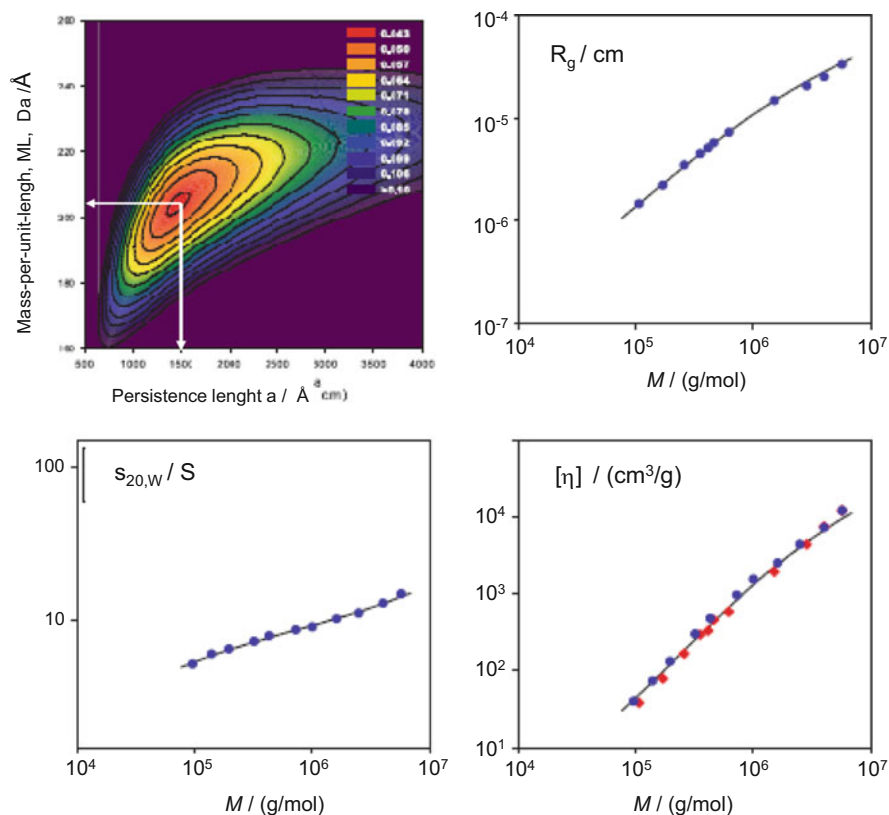


**Fig. 11.10** Multi-HYDFIT fit of experimental data and calculated values for three properties of schizophyllan.  $P = 1500 \text{ \AA}$ ,  $M_L = 205 \text{ Da/ \AA}$ ,  $d = 23 \text{ \AA}$  (Amorós et al. 2011). The contour plot displays  $\Delta$  vs.  $P$  and  $M_L$ , showing the position of the best-fitting minimum

one of them, I choose the analysis of properties of a very stiff polysaccharide: schizophyllan. Data for four properties (Yanaki et al. 1980, Kashiwagi et al. 1981) covering two decades in molecular weight were globally fitted by Multi-HYDFIT, collecting data in a single file, and running the program, which took barely 2 min (Fig. 11.10).

## 11.5 Conclusions

The HYDRO suite – which is the fruit of nearly 40 years of the authors’ work – provides a collection of tools that have been consistently developed, in the context of the theory of hydrodynamic interaction of bead models. Utilities are available for both rigid and flexible structure, with the added bonus of some programs for

the inverse problem of structural determination from solution properties. Ample documentation, including users' guides and worked examples, are available for all the programs, which can be downloaded freely and anonymously from our web site (García de la Torre 2014).

**Acknowledgments** This chapter was written while the author was supported by grant CTQ2012-33717 from *Ministerio de Ciencia y Competitividad*, including FEDER funds. The author's group is one of the groups of excellence in the Region of Murcia, supported by *Fundación Séneca*, grant 04531/GERM/06 and grant 19353/PI/14.

## References

- Allison SA (1986) Brownian dynamics simulation of wormlike chains. Fluorescence depolarization and depolarized light scattering. *Macromolecules* 19:118–124
- Allison SA (1998) The primary electroviscous effect of rigid polyions of arbitrary shape and charge distributions. *Macromolecules* 31:4464–4474
- Allison SA (1999) Low Reynolds number transport properties of axisymmetric particles employing stick and slip boundary conditions. *Macromolecules* 32:5304–5212. Addition/Correction: (1999) 32:7710–7710
- Allison SA, McCammon JA (1984) Transport properties of rigid and flexible macromolecules by Brownian dynamics simulation. *Biopolymers* 23:167–187
- Amorós D, Ortega A, Harding SE, García de la Torre J (2010) Multi-scale calculation and global-fit analysis of hydrodynamic properties of biological macromolecules: determination of the overall conformation of antibody IgG molecules. *Eur Biophys J* 39:361–370
- Amorós D, Ortega A, García de la Torre J (2011) Hydrodynamic properties of wormlike macromolecules: Monte Carlo simulation and global analysis of experimental data. *Macromolecules* 44:5788–5797
- Aragón S (2004) A precise boundary element method for macromolecular transport properties. *J Comput Chem* 25:1191–1205
- Bernadó P, Blackledge M (2009) A self-consistent description of the conformational behaviour of chemically denaturated proteins from NMR and small angle scattering. *Biophys J* 97:2839–2845
- Binder K (ed) (1995) Monte Carlo and molecular dynamics simulations in polymer science. Oxford University Press, New York
- Bloomfield VA, Filson DP (1968) Shell model calculations of translational and rotational frictional coefficients. *J Polym Sci Part C* 25:73–83
- Bloomfield VA, Dalton WO, Van Holde KE (1967) Frictional coefficients of multisubunit structures. I. Theory. *Biopolymers* 5:135–148
- Brookes E, Demeler B, Rocco M (2010) Developments in the US-SOMO bead modeling suite: new features in the direct residue-to-bead method, improved grid routines, and influence of accessible surface area screening. *Macromol Biosci* 10:746–753
- Carrasco B, García de la Torre J (1999a) Hydrodynamic properties of rigid particles. Comparison of different modelling and computational procedures. *Biophys J* 76:3044–3057
- Carrasco B, García de la Torre J (1999b) Improved hydrodynamic interaction in macromolecular bead models. *J Chem Phys* 111:4817–4826
- Carrasco B, García de la Torre J, Davis KG, Jones S, Athwal D, Walters C, Burton DR, Harding S (2001) Crystalhydrodynamics for solving the hydration problem for multi-domain proteins: open physiological conformations for human IgG. *Biophys J* 93:181–196

- Clementi C, Nyemeyer H, Onuchic J (2000) Topological and energetic factors: what determines the structural details of the transition state ensemble and “En-route” intermediates for protein folding? An investigation for small globular proteins. *J Mol Biol* 298:937–953
- del Río EG, Rodríguez Schmidt R, Freire JJ, Hernández Cifre JG, García de la Torre J (2009) A multiscale scheme for the simulation of conformational and solution properties of some dendrimer molecules. *J Am Chem Soc* 131:8549–8556
- Díaz FG, Iniesta A, García de la Torre J (1987) Brownian dynamics simulation of rotational correlation functions of simple rigid models. *J Chem Phys* 87:6021–6027
- Ermak DL, McCammon JA (1978) Brownian dynamics with hydrodynamic interactions. *J Chem Phys* 69:1352–1360
- Fernandes MX, Bernadó P, Pons M, García de la Torre J (2001) An analytical solution to the problem of the orientation of rigid particles by planar obstacles. Application to membrane systems and to the calculation of dipolar couplings in protein NMR Spectroscopy. *J Am Chem Soc* 123:12037–12047
- Fernandes MX, Ortega A, López Martínez MC, García de la Torre J (2002) Calculation of hydrodynamic properties of small nucleic acids from their atomic structures. *Nucleic Acids Res* 30:1782–1788
- Fixman M (1986) Translational diffusion of chain polymers. I. Improved variational bounds. *J Chem Phys* 84:4080–4086
- García de la Torre J (2001a) Hydration from hydrodynamics. General considerations and applications of bead modelling to globular proteins. *Biophys Chem* 63:159–170
- García de la Torre J (2001b) Building hydrodynamic bead-shell models for rigid particles of arbitrary shape. *Biophys Chem* 94:265–274
- García de la Torre J (2007) Dynamic electro-optic properties of macromolecules and nanoparticles in solution. A review of computational and simulation methodologies. *Coll Surf B* 56:4–15
- García de la Torre J (2014) <http://leonardo.inf.um.es/macromol/>. Accessed 15 Apr 2014
- García de la Torre J, Bloomfield VA (1977a) Hydrodynamic properties of macromolecular complexes. I. Translation. *Biopolymers* 16:1747–1763
- García de la Torre J, Bloomfield VA (1977b) Hydrodynamic properties of macromolecular complexes. III. Bacterial viruses. *Biopolymers* 16:1779–1793
- García de la Torre J, Bloomfield VA (1981) Hydrodynamic properties of complex, rigid, biological macromolecules. Theory and applications. *Q Rev Biophys* 14:81–139
- García de la Torre J, Carrasco B (2002) Hydrodynamic properties of rigid macromolecules composed of ellipsoidal and cylindrical subunits. *Biopolymers* 63:163–167
- García de la Torre J, Harding SE (2013) Hydrodynamic modelling of protein conformation in solution: ELLIPS and HYDRO. *Biophys Rev* 5:195–206
- García de la Torre J, Horta A (1976) Sedimentation coefficient and X-Ray scattering of double-helical model for deoxyribonucleic acid. *J Phys Chem* 80:2028–2035
- García de la Torre J, Freire JJ, Horta A (1975) A bead and spring model for the stiffness of DNA. *Biopolymers* 14:1327–1335
- García de la Torre J, Jiménez A, Freire JJ (1982) Monte Carlo calculation of hydrodynamic properties of freely jointed, freely rotating and real polymethylene chains. *Macromolecules* 15:148–154
- García de la Torre J, Navarro S, López Martínez MC, Díaz FG, López Cascales JJ (1994) HYDRO: a computer software for the prediction of hydrodynamic properties of macromolecules. *Biophys J* 67:530–531
- García de la Torre J, Carrasco B, Harding SE (1999) Calculation of NMR relaxation, covolume and scattering-related properties of bead models using the SOLPRO computer program. *Eur Biophys J* 28:119–132
- García de la Torre J, Huertas ML, Carrasco B (2000a) Calculation of hydrodynamic properties of globular proteins from their atomic-level structure. *Biophys J* 78:719–730
- García de la Torre J, Huertas ML, Carrasco B (2000b) HYDRONMR: prediction of NMR relaxation of globular proteins from atomic-level structures and hydrodynamic calculations. *J Magn Reson* 147:138–146

- García de la Torre J, Llorca O, Carrascosa JL, Valpuesta JM (2001) HYDROMIC: prediction of hydrodynamic properties of rigid macromolecular structures obtained from electron microscopy. *Eur Biophys J* 30:457–462
- García de la Torre J, Ortega A, Pérez Sánchez HE, Hernández Cifre JG (2005) MULTIHIDRO and MONTEHYDRO: conformational search and Monte Carlo calculation of solution properties of rigid and flexible macromolecular models. *Biophys Chem* 116:12–128
- García de la Torre J, del Rio Echenique G, Ortega A (2007) Calculation of rotational diffusion and intrinsic viscosity of bead models for macromolecules and nanoparticles. *J Phys Chem B* 111:955–961
- García de la Torre J, Hernández Cifre JG, Ortega A, Rodríguez Schmidt R, Fernandes MX, Pérez Sánchez HE, Pamies R (2009) SIMUFLEX: algorithms and tools for simulation of the conformation and dynamics of flexible molecules and nanoparticles in dilute solution. *J Chem Theory Comput* 5:2606–2618
- García de la Torre J, Ortega A, Amorós D, Rodríguez Schmidt R, Hernández Cifre JG (2010a) Methods and tools for the prediction of hydrodynamic coefficients and other solution properties of flexible macromolecules in solution. A tutorial minireview. *Macromol Biosci* 10:721–730
- García de la Torre J, Amorós D, Ortega A (2010b) Intrinsic viscosity of bead models for macromolecules and nanoparticles. *Eur Biophys J* 39:381–388
- Gregory L, Davis KG, Sheth B, Boyd J, Jefferis R, Naves D, Burton K (1987) The solution conformations of the subclasses of human IgG deduced from sedimentation and small angle X-ray scattering studies. *Molec Immunol* 24:821–829
- Hagerman P, Zimm BH (1981) Monte Carlo approach to the analysis of the rotational diffusion of wormlike chains. *Biopolymers* 10:1481–1502
- Harding SE, Horton JC, Coelfen H (1997) The ELLIPS suite of macromolecular conformation algorithms. *Eur Biophys J* 25:347–359
- Harding SE, Horton JC, Jones S, Thornton JM, Winzor D (1999) COVOL: an interactive program for evaluating second virial coefficients from the triaxial shape or dimensions of rigid macromolecules. *Biophys J* 76:2434–2438
- Hiemenz PC, Lodge TP (2007) *Polymer chemistry*, 2nd edn. CRC Press, Boca Raton
- ImageScience (2014) <https://www.imagescience.de/em2em.html>. Accessed 1 May 2014
- Iniesta A, Diaz FG, García de la Torre J (1988) Transport properties of rigid bent-rod macromolecules and semiflexible broken rods in the rigid body approximation. *Biophys J* 54:269–275
- Kashiwagi Y, Norisuye T, Fujita H (1981) Triple helix of schizophyllum commune polysaccharide in dilute solution. 4. Light scattering and viscosity in dilute sodium hydroxide. *Macromolecules* 14:1220–1225
- Kirkwood JG, Auer PL (1951) The visco-elastic properties of solutions of rod-like macromolecules. *J Chem Phys* 19:281–287
- Kirkwood JG, Riseman J (1948) The intrinsic viscosities and diffusion constants of flexible macromolecules in solution. *J Chem Phys* 16:565–573
- Kleywegt GJ (1997) Validation of protein models from  $C^\alpha$  coordinates alone. *J Mol Biol* 273:371–376
- Krzeminski M, Marsh JA, Neale C, Choy WY, Forman-Kay JD (2013) Characterization of disordered proteins with ENSEMBLE. *Bioinformatics* 29:398–399
- Lu Y, Harding S, Michaelsen T, Longman E, Davis KG, Ortega A, Grossman G, Sandler I, Garcia de la Torre J (2007) Solution conformation of wild type and mutant IgG3 and IgG4 immunoglobulins using crystallohydrodynamics: possible implications for complement activation. *Biophys J* 93:3733–3744
- McCammon JA, Deutch JM (1976) Frictional properties of nonspherical multisubunit structures. Application to tubules and cylinders. *Biopolymers* 15:1397–1408
- Nakajima H, Wada Y (1977) A general method for the evaluation of diffusion constant, dilute-solution viscoelasticity and the complex dielectric constant of a rigid macromolecule with an arbitrary configuration. *Biopolymers* 16:875–893

- Ortega A, García de la Torre J (2007) Equivalent radii and ratios of radii from solution properties as indicators of macromolecular shape, conformation and flexibility. *Biomacromolecules* 8:2464–2475
- Ortega A, Amorós D, García de la Torre J (2011a) Prediction of hydrodynamic and other solution properties of rigid proteins from atomic- and residue-level models. *Biophys J* 101:892–898
- Ortega A, Amorós D, García de la Torre J (2011b) Global fit and structure optimization of flexible and rigid macromolecules and nanoparticles from analytical ultracentrifugation and other dilute solution properties. *Methods* 54:115–123
- Pavlov GM, Korneeva EV, Smolina NA, Schubert US (2010) Hydrodynamic properties of cyclodextrin molecules in dilute solution. *Eur Biophys J* 39:371–379
- Perkins TT, Smith DE, Chu S (1997) Single polymer dynamics in an elongational flow. *Science* 276:2016–2021
- Rai N, Nollman M, Rocco M (2005) SOMO (Solution Modeller) differences between X-ray and NMR-derived bead models suggest a role for side chain flexibility in protein dynamics. *Structure* 13:722–734
- Rodríguez Schmidt R, Hernández Cifre JG, García de la Torre J (2011) Comparison of Brownian dynamics algorithms with hydrodynamic interaction. *J Chem Phys* 135:084116
- Rodríguez Schmidt R, Hernández Cifre JG, García de la Torre J (2012) Translational diffusion coefficients of macromolecules. *Eur J Phys Educ* 35:130
- Rotne J, Prager S (1969) Variational treatment of hydrodynamic interaction on polymers. *J Chem Phys* 50:4831–4837
- Rubinstein M, Colby RH (2003) *Polymer physics*. Oxford University Press, Oxford
- Schlagberger X, Netz R (2008) Anomalous sedimentation of self-avoiding flexible polymers. *Macromolecules* 41:1861–1871
- Schuck P (2000) Size-distribution analysis of macromolecules by sedimentation velocity ultracentrifugation and Lamm equation modeling. *Biophys J* 78:1606–1619
- Serdyuk IN, Zaccai NR, Zaccai J (2007) *Methods in molecular biophysics*. Cambridge University Press, Cambridge
- Sobolev V, Sorokine A, Prilusky J, Abola EE, Edelman M (1999) Automated analysis of interatomic contacts in proteins. *Bioinformatics* 15:327–332
- Voth GA (ed) (2009) *Coarse-graining of condensed phase and biomolecular systems*. CRC Press, Boca Raton
- Wang N, Huber G, McCammon JA (2013) Assessing the two-body diffusion tensor calculated by bead models. *J Chem Phys* 138:204117
- Yamakawa H (1970) Transport properties of polymer chains in dilute solution: hydrodynamic interaction. *J Chem Phys* 53:436–443
- Yamakawa H, Fujii M (1973) Translational friction coefficient of wormlike chains. *Macromolecules* 6:407–415
- Yamakawa H, Fujii M (1974) Intrinsic viscosity of wormlike chains. Determination of the shift factor. *Macromolecules* 7:128–135
- Yamakawa H, Tanaka G (1972) Translational diffusion coefficients of rodlike polymers: application of the modified Oseen tensor. *J Chem Phys* 57:1537–1546
- Yamakawa H, Yamaki J (1972) Translational diffusion coefficients of plane-polygonal polymers: application of the modified Oseen tensor. *J Chem Phys* 57:1542–1546
- Yanaki T, Norisuye T, Fujita H (1980) Triple helix of schizophyllum commune polysaccharide in dilute solution. 3. Hydrodynamic properties. *Macromolecules* 13:1462–1466
- Zimm BH (1974) Anomalies in sedimentation. IV. Decrease in sedimentation coefficients of chains at high fields. *Biophys Chem* 1:279–292
- Zimm BH (1980) Chain molecule hydrodynamics by the Monte-Carlo method and the validity of the Kirkwood-Riseman approximation. *Macromolecules* 13:592–602
- Zimm BH, Schumaker VN, Zimm CB (1976) Anomalies in sedimentation. V. Chains at high fields, practical consequences. *Biophys Chem* 5:265–270